Fractional approach to evolution of the magnetic field lines near the magnetic null points

Hasan Durmaz*, Zehra Özdemir†, Yadigar Sekerci‡

Department of Mathematics, Arts and Science Faculty, Amasya University, 05189 Amasya, Turkey

Abstract

In this work, the magnetic reconnection model near null points in 3D space will be investigated using fractional calculations in the 3D magnetohydrodynamic framework. For the initial magnetic configuration (without external currents), we reformulated the numerically solved boundary initial value problem using fractional calculations. We studied the 3D Magnetic reconnection states and the behavior of the magnetic field around the null point and the null line. We also analyzed the fractional significance of charged particle motions in Killing magnetic fields. Moreover, the obtained results were visualized, and a comparison was made between the results obtained from integer and fractional calculations.

MSC: 26A33; 97M50; 81T80; 97MXX; 53A04; 53B50; 11R52; 16H05; 32A07.
Keywords: Fractional derivatives, Numerical simulation, Computational modeling, Applications to physics, Vector fields, Magnetic flows.

1 Introduction

The huge variety of phenomena described by the equations of magnetic hydrodynamics, and the processes of reconnection of magnetic field lines in a highly conductive plasma are of particular interest. Magnetic reconnection can occur in those areas where the lines of force come close to each other in different directions of the magnetic field, i.e. in areas with high electric current density. In external inhomogeneous magnetic fields, the convergence of opposite lines of force, magnetic reconnection processes, and the concentration of electric current are possible in the vicinity of special lines of force, the most famous examples of which are the zero lines of the magnetic field. Such configurations and magnetohydrodynamic flows in them began to be discussed in the literature in [1–4].

Fractional differential equations have become a rather attractive research area due to having a vast of application areas. We can give some of these application areas in medicine [5], pharmacokinetics [6, 7], physics [8–12], biology [13, 14], epidemic models [15–17], nuclear magnetic resonance systems [18], [19–23].

* E–mail: hasan05durmaz@gmail.com (H. Durmaz)
† E–mail: zehra.ozdemir@amasya.edu.tr (Z. Özdemir)
‡ E–mail: yadigar.firat@amasya.edu.tr (Y. Sekerci)

The fractional derivative was born as a result of L'Hospital's search for an answer to Leibniz's question of the meaning of the $1/2$th order. First, in a serious sense, Caputo started with the fractional derivative. The most important advantage of Caputo over Riemann-Liouville is that the fractional derivative of a constant is zero and the initial conditions have integer order. In recent years, fractional analysis has made great progress both in theory and in practice [28–31]. One of the advantages of fractional derivatives over integer derivatives is that they are nonlocal and have a memory effect. There are many studies explaining that applications of fractional derivatives give more precise results than classical applications [5, 15–17]. Also, we need some numerical methods [32, 33, 35, 36] since it does not seem possible to find analytical solutions to fractional differential equations.

Generally speaking, fractional applications are formulated according to a more complex model than an integer one, so to obtain information about the geometry of the model, they can be plotted and the corresponding model analyzed. This approach is given by Milici and Machado, [37]. In [38,39], Has et al. investigated the many special curves by using conformable fractional derivatives. Electromagnetic curves and some special magnetic curves with the help of fractional derivatives, [24, 26, 27].

2 Three-dimensional null points with fractional calculus

In this section, firstly, we introduce the three-dimensional null point characterizations and then we investigate the behavior of the magnetic field lines near the null (neutral) points of the magnetic field via fractional calculus. Furthermore, we will visualize the results of integer and fractional derivatives representing the behavior of magnetic field lines near the null point through mathematical programs.

Null points are locations where the magnetic field vanishes, that is E singular or $v\perp$ singular. A null point can occur whether the magnetized medium is a conducting plasma or a neutral gas. Through this work, we use the notion for the magnetic field, denoted as B. Since the magnetic field is a divergence free vector field, it satisfies the Gauss law $\nabla.B = 0$. The magnetohydrodynamic (MHD) form of Ohm's law is given as follows:

$$E + v \times B = \eta J,$$

where E, v, B, J and η denote electric field, velocity, magnetic field, current density and vacuum permeability, respectively.

The behavior of the magnetic field lines near the null points can be characterized by the Taylor expansion (for $x = 0$) of the magnetic field B. Thus we can write $B(x) = (\delta B)x$, here $\delta B = [\frac{\partial B_i}{\partial x_i}]$, $i \in \{1,2,3\}$.

The matrix δB has three eigenvalues λ_1, λ_2, λ_3. Through these eigenvalues, the behaviour of the magnetic field lines near the null points is given as follows:

1. Let us take one of the eigenvalues λ_1 without breaking the generality, if $\lambda_1 = 0$ then the sum of the other two eigenvalues λ_2, λ_3 must be zero.

i. When λ_2 and λ_3 are real, this is an $X - point$.

ii. When λ_2 and λ_3 are complex, this is an $O - point$.

2. If all three eigenvalues λ_1, λ_2, λ_3 are real then we have

i. When they are $(+,-,-)$, it is called as $type\ A$.

ii. When they are $(-,+,+)$, it is called as *type B*.

3. One of the eigenvalues is real (say λ_1) and the other two eigenvalues are complex.

i. If $\lambda_1 > 0$ then the null called as *type* A_s.

ii. If $\lambda_1 < 0$ then the null called as *type* B_s (see for details, [40]).

In three-dimensional space, the magnetic field line associated with B can be obtained as the solution of the following differential equation

$$\frac{\partial x}{\partial t} = B_x,\ \frac{\partial y}{\partial t} = B_y,\ \frac{\partial z}{\partial t} = B_z \text{ or } \frac{\partial r}{\partial t} = B.$$

Also, the differential equation for magnetic field lines of the magnetic field $B = B_x\partial_x + B_y\partial_y + B_z\partial_z$ given as

$$\frac{dx}{B_x} = \frac{dy}{B_y} = \frac{dz}{B_z}.$$

Then, we write the most general expression for a current-free field:

$$B = (a_1x + b_1y + c_1z)\partial_x + (a_2x + b_2y + c_2z)\partial_y + (a_3x + b_3y - (a_1 + b_2)z)\partial_z. \tag{1}$$

Then the fractional differential equations satisfy

$$D^\alpha x = B_x, D^\alpha y = B_y, D^\alpha z = B_z, \tag{2}$$

where the fractional derivative D_α defined as Caputo fractional derivative of order $0 < \alpha \leq 1$ for a smooth function $f(t)$ is defined as follows

$$D_\alpha f(t) = \frac{1}{\Gamma(1-\alpha)} \int_0^t \frac{1}{(t-x)^\alpha} f'(x)dx, \tag{3}$$

and a_i, b_i, c_i for $i = \{1,2,3\}$ satisfy the conditions $b_1 = a_2$, $c_1 = a_3$, $c_2 = b_3$, $c_3 = -(a_1 + b_2)$, are five independent parameters. This field is characterized by a symmetric matrix

$$\delta B = \begin{bmatrix} a_1 & b_1 & c_1 \\ a_2 & b_2 & c_2 \\ a_3 & b_3 & -(a_1+b_2) \end{bmatrix}$$

The characteristic equation determining its eigenvalues has the form

$$P(\lambda) = \lambda^3 - p\lambda - q = 0$$

where

$$p = a_1^2 + a_1b_2 + b_2^2 + b_1^2 + c_2^2 + c_1^2, \tag{4}$$

$$q = 2b_1b_3c_1 + (b_1^2 - a_1b_2)(a_1 + b_2) - (a_1c_2^2 + b_2c_1^2). \tag{5}$$

We construct an orthonormal basis $\{e_1, e_2, e_3\}$ from the eigenvectors of the matrix δB and write in magnetic field

$$B = \lambda_1\xi e_1 + \lambda_2\eta e_2 + \lambda_3\nu e_2$$

where λ_i, $i = 1,2,3$, are the eigenvalues of the matrix δB, the sum of which is equal to zero

$$\lambda_1 + \lambda_2 + \lambda_3 = 0, \tag{6}$$

and ξ, λ, ν are some constants.

Next, we provide some motivated examples and visualize them using mathematical programs. In Figures 2-5, the red-colored curves correspond to the fractional solutions, while the black-colored curves represent the integer solutions of the corresponding equations.

Example 2.1. Firstly, we take the circular magnetic field $B = z\partial_x - x\partial_z$. In three-dimensional space, the magnetic field line associated with B can be obtained as the solution of the following differential equation

$$\frac{\partial x}{\partial t} = z,\ \frac{\partial y}{\partial t} = 0,\ \frac{\partial z}{\partial t} = -x. \tag{7}$$

The integer solution of the equation (7) obtained as,

$$X(t) = (a_1 \cos t + a_2 \sin t)\partial_x + a_3\partial_y + (a_2 \cos t - a_1 \sin t)\partial_z, \tag{8}$$

where a_i, $i = \{1,2,3\}$ are real constants. The fractional solution of the equation (7) is computed as follows;

$$\begin{aligned} x(t) &= t^{2\alpha-1}E_{2\alpha,2\alpha}\left(-t^{2\alpha}\right) + t^{\alpha-1}E_{2\alpha,\alpha}\left(-t^{2\alpha}\right), && (9)\\ y(t) &= \frac{t^{\alpha-1}}{\Gamma(\alpha)}, && (10)\\ z(t) &= -t^{2\alpha-1}E_{2\alpha,2\alpha}\left(-t^{2\alpha}\right) + t^{\alpha-1}E_{2\alpha,\alpha}\left(-t^{2\alpha}\right), && (11) \end{aligned}$$

where $\Gamma(x) = \int_0^\infty t^{x-1}e^{-t}dt$, $x \in \mathbb{R}^+$ and $E_{i,j}(x) = \sum_{k=0}^{\infty} \frac{x^k}{\Gamma(ik+j)}$, $i, j > 0, x \in \mathbb{C}$.

Then we obtain the following magnetic field lines. These are illustrated in Figure 1.

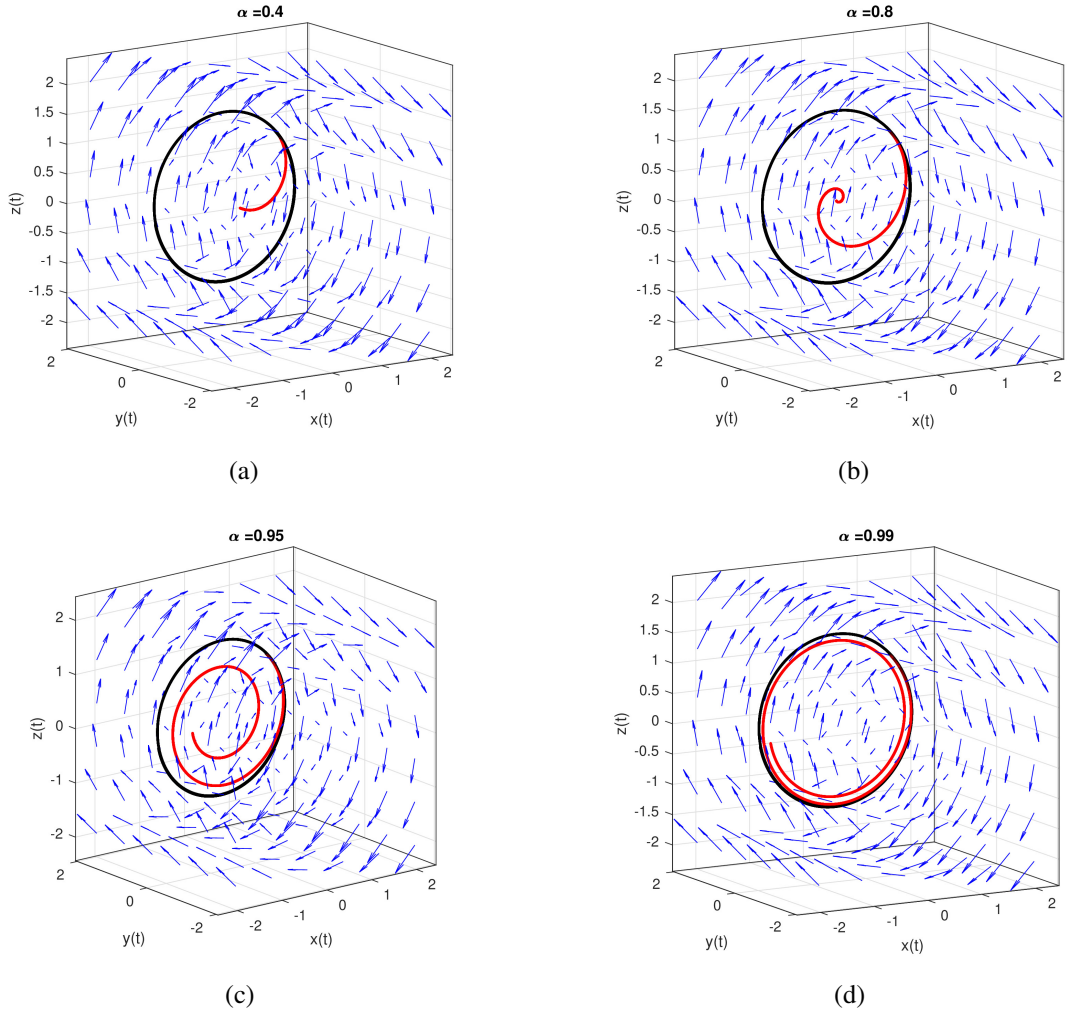

(a) (b) (c) (d)

Figure 1: Behavior of the magnetic field lines near the null point (O-point) for $\alpha = 0.4$, $\alpha = 0.8$, $\alpha = 0.95$, $\alpha = 0.99$ for given initials $x(0) = 1, y(0) = 1, z(0) = 1$.

Example 2.2. Secondly, we take the hyperbolic magnetic field $B = z\partial_x + x\partial_z$. Then the magnetic field line associated with B can be obtained as the solution of the following differential equation

$$\frac{\partial x}{\partial t} = z, \ \frac{\partial y}{\partial t} = 0, \ \frac{\partial z}{\partial t} = x. \tag{12}$$

The integer solution of the equation (12) obtained as

$$X(t) = (a_1 \cosh t + a_2 \sinh t)\partial_x + a_3\partial_y + (a_2 \cosh t + a_1 \sinh t)\partial_z. \tag{13}$$

The fractional solution of the equation (12) is obtained by

$$x(t) = t^{\alpha-1} E_{\alpha,\alpha}(t^\alpha), \tag{14}$$

$$y(t) = \frac{t^{\alpha-1}}{\Gamma(\alpha)}, \tag{15}$$

$$z(t) = t^{\alpha-1} E_{\alpha,\alpha}(t^\alpha). \tag{16}$$

Then we obtain the following magnetic field lines. These are illustrated in Figure 2.

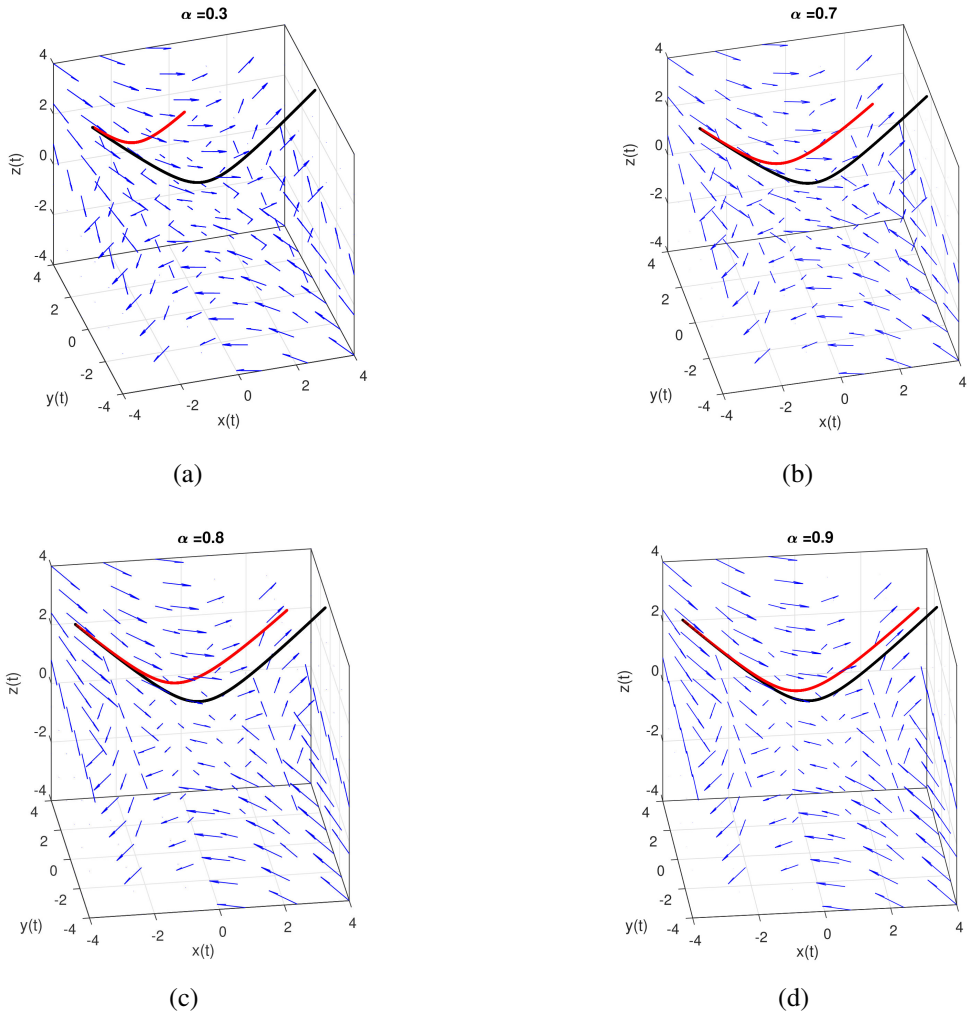

(a) (b)

(c) (d)

Figure 2: Behavior of the magnetic field lines near the null point (X-point) for $\alpha = 0.3$, $\alpha = 0.7$, $\alpha = 0.8$, $\alpha = 0.9$ for given initials $x(0) = -5.9, y(0) = 0, z(0) = 6$.

Example 2.3. Finally, we take the spiral magnetic field $B = (-x+y)\partial_x + (-x+2y-2z)\partial_y + (2y-z)\partial_z$. In three-dimensional space, the magnetic field line associated with B can be obtained as the solution of the following differential equation

$$\frac{\partial x}{\partial t} = -x+y, \ \frac{\partial y}{\partial t} = -x+2y-2z, \ \frac{\partial z}{\partial t} = 2y-z. \tag{17}$$

One of the integer solutions of the equation (17) obtained as

$$\gamma(t) = \exp(\frac{t}{2}) \begin{pmatrix} (\frac{3-\sqrt{11}}{10})\cos\frac{\sqrt{11}t}{2} + (\frac{3+\sqrt{11}}{10})\sin\frac{\sqrt{11}t}{2}, \\ \cos\frac{\sqrt{11}t}{2} + \sin\frac{\sqrt{11}t}{2}, \\ (\frac{3-\sqrt{11}}{5})\cos\frac{\sqrt{11}t}{2} + (\frac{3+\sqrt{11}}{5})\sin\frac{\sqrt{11}t}{2} \end{pmatrix}.$$

The fractional solution of the (17) is calculated as Fractional version of example 2.3

$$x(t) = t^{3\alpha-1}\sum_{n=0}^{\infty}\sum_{k=0}^{\infty}\frac{(-3)^n(-2)^k\binom{n+k}{k}}{\Gamma(2k\alpha+3(n+1)\alpha)}t^{\alpha(2k+3n)} + t^{\alpha-1}\sum_{n=0}^{\infty}\sum_{k=0}^{\infty}\frac{(-3)^n(-2)^k\binom{n+k}{k}}{\Gamma(2k\alpha+3(n+1)\alpha-2\alpha)}t^{\alpha(2k+3n)} \tag{18}$$

$$y(t) = -2t^{2\alpha-1}\sum_{n=0}^{\infty}\sum_{k=0}^{\infty}\frac{(-3)^n\binom{n+k}{k}}{\Gamma(k\alpha+2(n+1)\alpha-\alpha)}t^{\alpha(k+2n)} + t^{\alpha-1}\sum_{n=0}^{\infty}\sum_{k=0}^{\infty}\frac{(-3)^n\binom{n+k}{k}}{\Gamma(k\alpha+2(n+1)\alpha-\alpha)}t^{\alpha(k+2n)} \tag{19}$$

$$z(t) = -t^{3\alpha-1}\sum_{n=0}^{\infty}\sum_{k=0}^{\infty}\frac{(-3)^n(-2)^k\binom{n+k}{k}}{\Gamma(2k\alpha+3(n+1)\alpha)}t^{\alpha(2k+3n)} + t^{2\alpha-1}\sum_{n=0}^{\infty}\sum_{k=0}^{\infty}\frac{(-3)^n(-2)^k\binom{n+k}{k}}{\Gamma(2k\alpha+3(n+1)\alpha-\alpha)}t^{\alpha(2k+3n)} \tag{20}$$

$$+ t^{\alpha-1}\sum_{n=0}^{\infty}\sum_{k=0}^{\infty}\frac{(-3)^n(-2)^k\binom{n+k}{k}}{\Gamma(2k\alpha+3(n+1)\alpha-2\alpha)}t^{\alpha(2k+3n)}$$

Then we obtain the following magnetic field lines. These are illustrated in Figure 3.

One of the eigenvalues of the matrix associated with the magnetic field B is real and the other two are complex numbers. Thus, the resulting magnetic field lines are spirals.

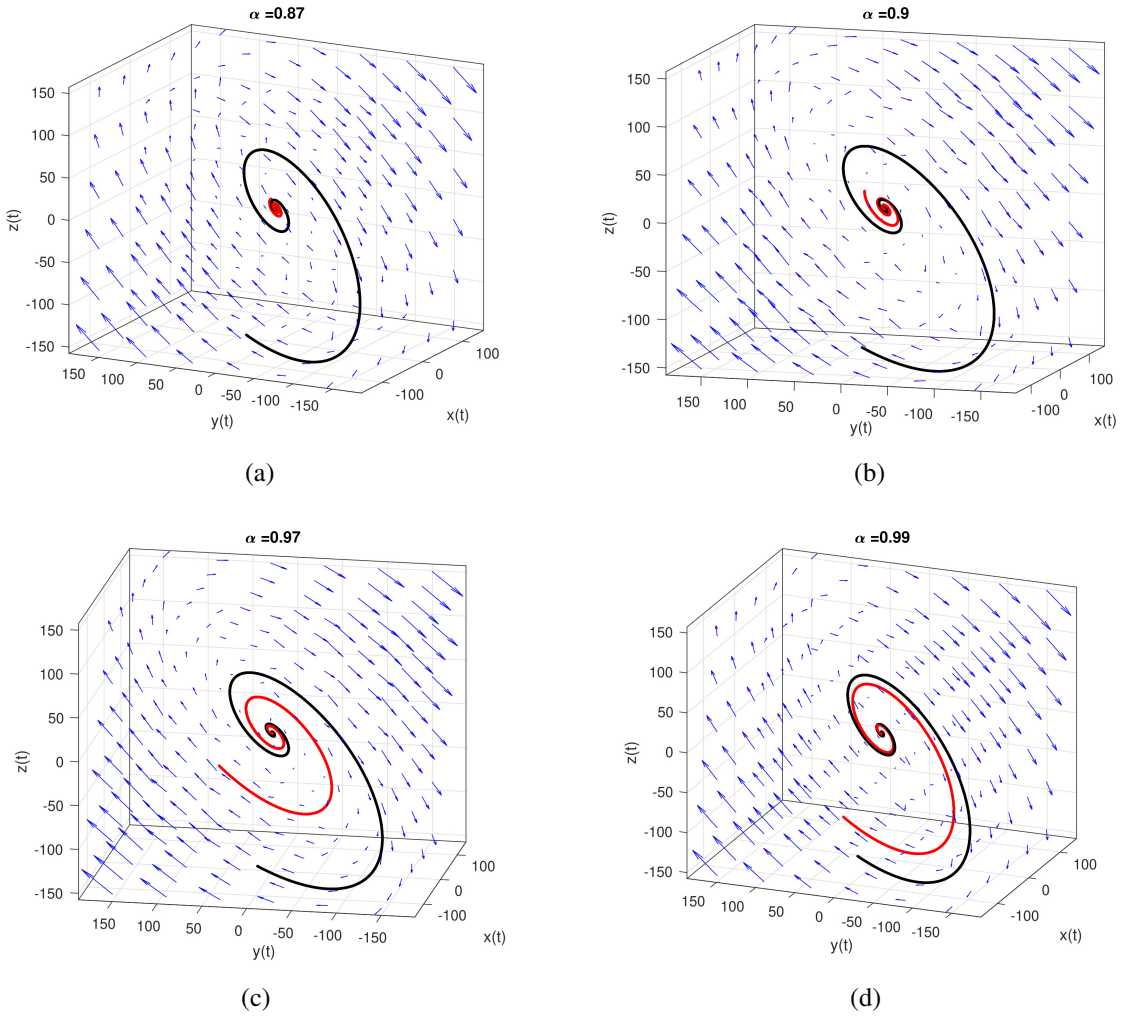

(a) (b) (c) (d)

Figure 3: Behavior of the magnetic field lines near the null point (As or Bs-point) for $\alpha = 0.87$, $\alpha = 0.9$, $\alpha = 0.97$, $\alpha = 0.99$, for given initials $x(0) = 1, y(0) = 1, z(0) = 1$.

3 Magnetic reconnection near the neutral points

A divergence-free vector field (∇B=0) defined as a magnetic field. Since the Killing vector field are divergence free vector field, they define magnetic vector field called Killing magnetic vector field in three dimensional space. Magnetic reconnection is a basic process where the magnetic field becomes restructured in many areas of plasma physics. The global topology of the magnetic field changes at null points. Our approach was to model this restructuring using fractional techniques to better understand the evolution. Reconnection takes place in two dimensions at hyperbolic null points of the hyperbolic magnetic field (for example [40, 43] for review), which are commonly known as X-points (see Figures **??** and 4). The reconnection can be explained as follows: The magnetic field lines are carried towards the X-point by a plasma flow; where the field lines carried on either side of the zero point are broken as soon as they extend along the separators of the field. The flow then carries the reconnected magnetic field lines away from the X-point, whose endpoints

are now mutually connected in pairs.

Example 3.1. Let $B = x\partial_x + (py - jz)\partial_y - (p+1)z\partial_z$ be a magnetic field, then the magnetic field line associated with B can be obtained as the solution of the following differential equation

$$\frac{\partial x}{\partial t} = x,\ \frac{\partial y}{\partial t} = py - jz,\ \frac{\partial z}{\partial t} = -(p+1)z. \tag{21}$$

The integer solution of the equation (21) gives hyperbolic magnetic field,

$$X(t) = c_1 e^t \partial_x + c_2 e^{pt} \partial_y + c_3 e^{-(p+1)t} \partial_z. \tag{22}$$

The fractional solution of the equation (21) is obtained as

$$\begin{aligned} x(t) &= t^{\alpha-1} E_{\alpha,\alpha}(t^\alpha), && (23)\\ y(t) &= t^{\alpha-1} E_{\alpha,\alpha}(pt^\alpha), && (24)\\ z(t) &= \frac{t^{\alpha-1}}{p+2} E_{\alpha,\alpha}(t^\alpha) + \frac{p+1}{p+2} E_{\alpha,\alpha}(-(p+1)t^\alpha). && (25) \end{aligned}$$

Then we obtain the following magnetic field lines illustrated in Figure 4.

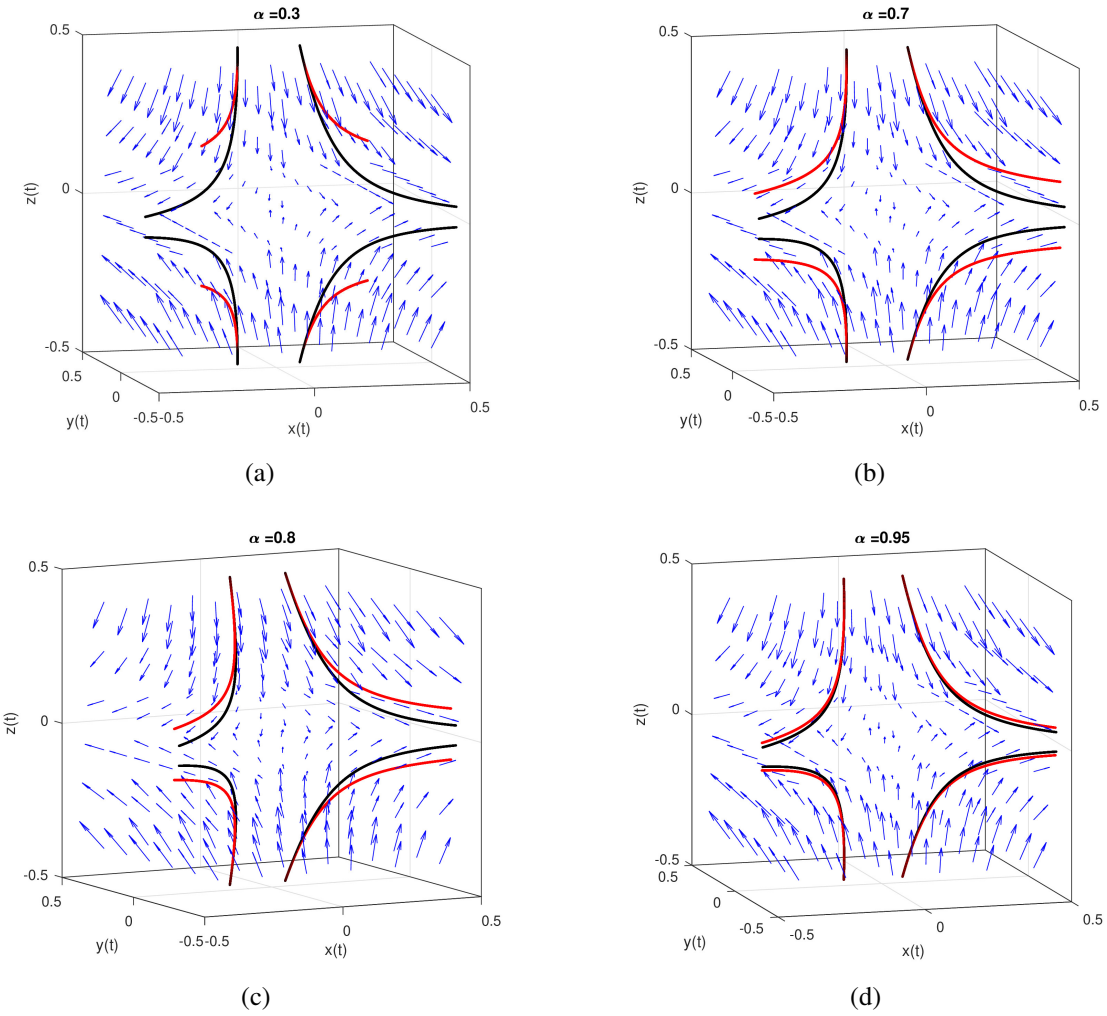

(a) (b) (c) (d)

Figure 4: Behavior of the magnetic field lines near the null point (A or B-point) for $\alpha = 0.3$, $\alpha = 0.7$, $\alpha = 0.8$, $\alpha = 0.95$ for given system parameters $B_0 = 0.8$; $L = 3$; $j = 1$; $p = 0.7$ and for given initials $x(0) = 0.1, y(0) = 0.1, z(0) = 0.5$.

4 Fractional meanings of the motion of a charged particle in the parallel Killing magnetic field

Magnetic curves are special curves most studies have done related to these curves (see, [44–50]) When a charged particle enters the magnetic field, a force called the Lorentz force occurs, the particle follows a trajectory called a magnetic curve in response to the Lorentz force. The magnetic field is closed 2-form which gives the following equation for all $X = (x_1, x_2, x_3)$, $Y = (y_1, y_2, y_3)$ is the form

$$g(F_L(X), Y) = F(X, Y). \tag{26}$$

In 3-dimensional spaces, since vector fields with zero-divergence define magnetic fields, the Lorentz force on the magnetic field vector B for all $X = (x_1, x_2, x_3)$ is Φ_L can be given by the

following formula:

$$\Phi_L(X) = B \times X. \tag{27}$$

The magnetic curves obtained from here are obtained as the solution of the following equation

$$\Phi_L(\mathbf{t}^\alpha) = B \times \mathbf{t}^\alpha = \nabla_{\mathbf{t}^\alpha}\mathbf{t}^\alpha, \tag{28}$$

where ∇ is the Levi-Civita connection, $\mathbf{t}^\alpha$ is the tangent vector of the magnetic field.

Let γ be a unit speed fractional magnetic curve associated with the magnetic field B if and only if B can be written as

$$B := \Omega\mathbf{t}^\alpha + \kappa\mathbf{b}^\alpha, \tag{29}$$

where $\mathbf{t}^\alpha$ tangent vector, $\mathbf{b}^\alpha$ binormal vector of γ, and Ω is a constant function of the angle at which the charged particle enters the magnetic field [24]. Now let's determine the magnetic curves associated with the parallel Killing vector field using fractional computation. Without compromising the generality, let us take the parallel Killing magnetic field $B = \partial_z$, then we get the following differential equations

$$\begin{aligned} D^\alpha(D^\alpha x(t)) &= D^\alpha y(t), \\ D^\alpha(D^\alpha y(t)) &= -D^\alpha x(t), \\ D^\alpha(D^\alpha z(t)) &= 0. \end{aligned} \tag{30}$$

The fractional solution of the equation (30) is obtained by

$$x(t) = \int (t^{2\alpha-1}E_{2\alpha,2\alpha}\left(-t^{2\alpha}\right) + t^{\alpha-1}E_{2\alpha,\alpha}\left(-t^{2\alpha}\right)), \tag{31}$$

$$y(t) = -\int (t^{2\alpha-1}E_{2\alpha,2\alpha}\left(-t^{2\alpha}\right) + t^{\alpha-1}E_{2\alpha,\alpha}\left(-t^{2\alpha}\right)), \tag{32}$$

$$z(t) = \int (\frac{t^{\alpha-1}}{\Gamma(\alpha)}). \tag{33}$$

Then we obtain the following magnetic field lines illustrated in both Figure 5 and Figure 6. In Figure 5, we show the behavior of the charged particle in the magnetic field B (blue) when the particle enters the magnetic field B with the perpendicular angle (resp. $\Omega = 0$). We can say that the particle follows a circular trajectory for the integer solutions and a spiral trajectory for fractional solutions. In Figure 6, we demonstrate the behavior of the charged particle in the magnetic field B when the particle enters the magnetic field B for all angles not equal to 90° (resp. $\Omega = const$). We can conclude that the particle follows a helical trajectory for the integer solutions and a spiral-helical trajectory for fractional solutions.

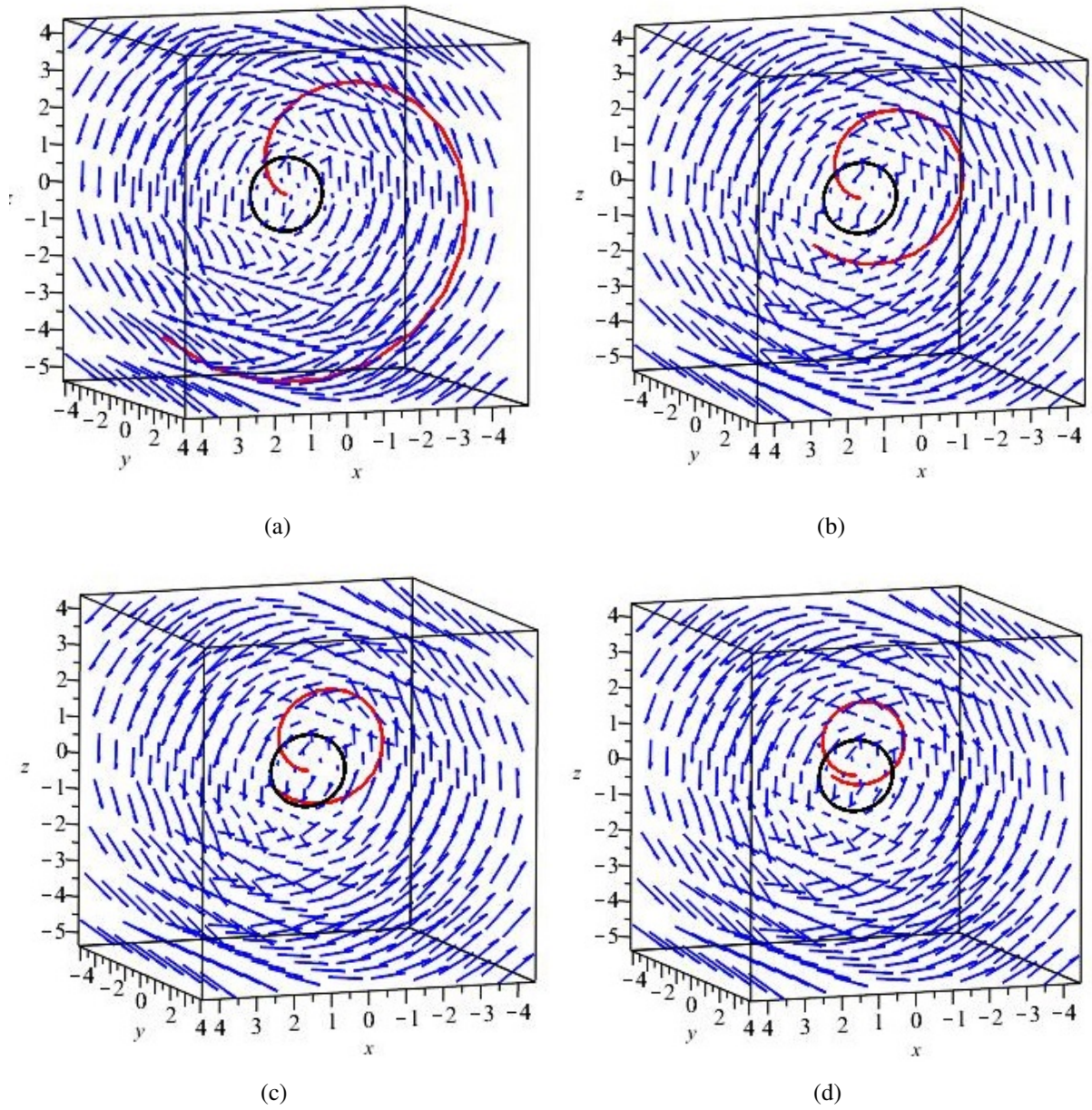

(a) (b)

(c) (d)

Figure 5: Circular charged particle trajectories of the magnetic field B for $\alpha = 0.1$, $\alpha = 0.5$, $\alpha = 0.7$, $\alpha = 0.9$ for given initials $x(0) = 0.1, y(0) = 0.1, z(0) = 0.5$. In figures, the black one is the integer solution of the equation (30).

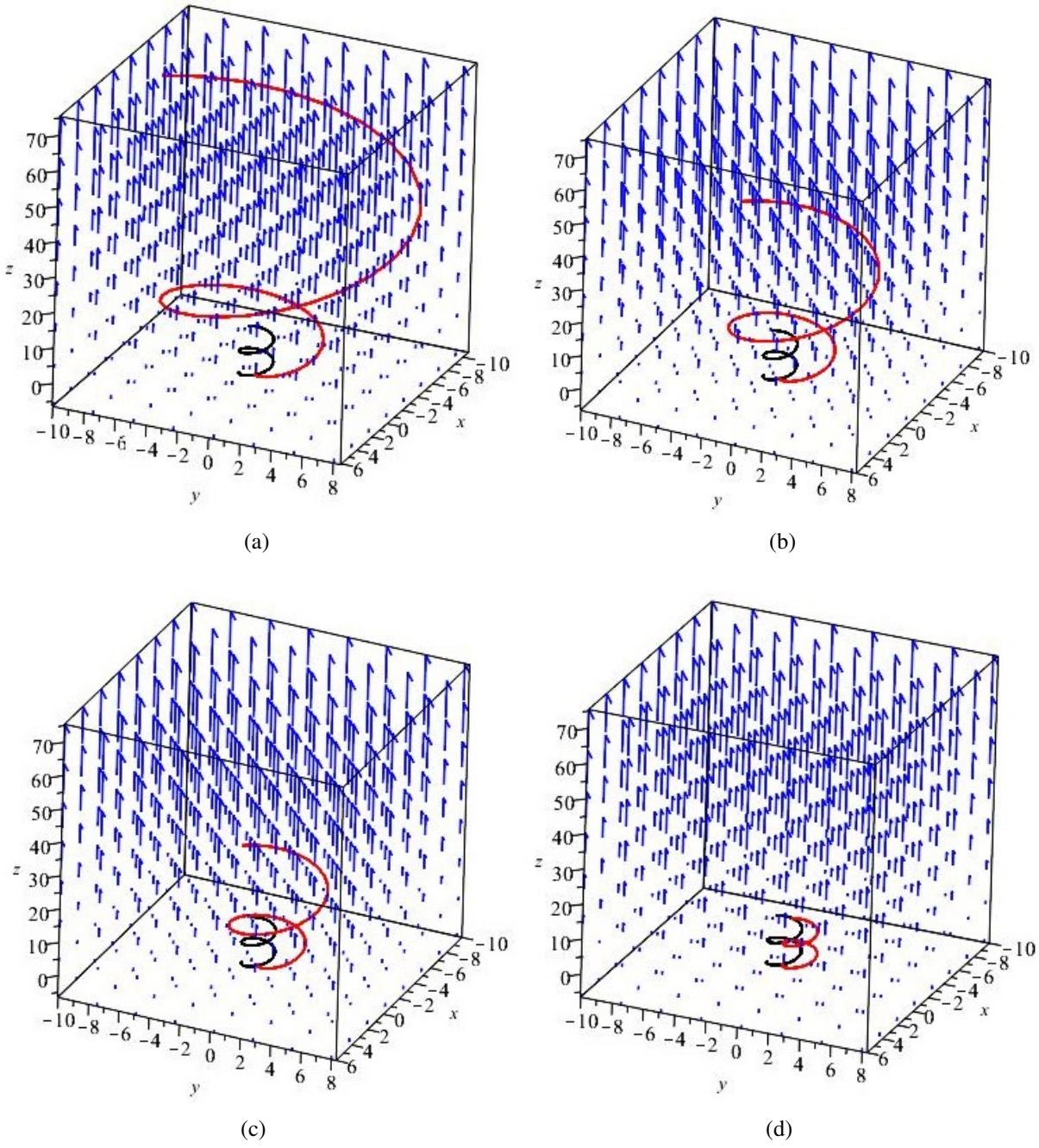

(a) (b)

(c) (d)

Figure 6: Charged particle trajectories of the magnetic field B for $\alpha = 0.005$, , $\alpha = 0.3$, $\alpha = 0.5$, $\alpha = 0.9$ for given initials $x(0) = 0.1, y(0) = 0.1, z(0) = 0.5$. In figures, the black one is the integer solution of the equation (30).

As seen in Figure 1, for a circular magnetic field lines associated with an O-point null point are obtained when $\alpha = 1$, while spiral magnetic field lines are obtained when α value is in the range of $0 < \alpha < 1$. In Figure 2, the effects of a magnetic field line acting as an X-point according to the α value in the fractional derivative. We show that the behavior around the null point is spiral according to the α value in the fractional derivative, they are (spiral (*As* or *Bs*)-point) visualized according to the α value in Figure 3. In addition, the magnetic reconnection around the null points

is examined with the help of the fractional derivative, and the results were drawn by comparing the initial magnetic field line in Figure 4. In section 4, the behavior of a charged particle in a parallel Killing magnetic field is interpreted with a fractional derivative. A charged particle follows a right circular-helix trajectory along a parallel magnetic field in Euclidean space. Moreover, the axis of this helix is the given parallel Killing vector field [44]. According to the results made with fractional derivative, while the value of α is in the range of $0 < \alpha < 1$, the particle follows a trajectory in the form of a spiral-helix curve. Again, the axis of this spiral-helix is parallel to the Killing vector field. The results obtained here are visualized in Figure 6. As a result, we can interpret the motion of a charged particle in a magnetic field of the fractional derivative when α value is in the range of $0 < \alpha < 1$ as follows: If the tangential vector field of the charged particle enters the magnetic field at right angles, the particle follows a circular trajectory in the magnetic field when $\alpha = 1$, while it follows a spiral-shaped trajectory when $0 < \alpha < 1$. If the tangential vector field of the charged particle enters the magnetic field at a constant angle (not right angle), while $\alpha = 1$, the particle follows a helix-shaped trajectory in the magnetic field, while at $0 < \alpha < 1$, it follows a spiral-helix-shaped trajectory.

5 Conclusions

In this paper, the effects of fractional calculus on the behavior of magnetic field lines around null points are investigated. Examined results are visualized with the help of mathematical programs. In practice, the fractional derivative method can be used to monitor the stages of the magnetic field lines that reach that procedure up until the first derivative is attained. Hence, it is possible to obtain that we are observing the evolution stages of magnetic field lines as they transition into the first derivative state through the utilization of the fractional derivative. After that, we examined charged-particle motions near the null points. So, we investigated the reconnection resulting from this point around the null point using the fractional analysis method. We visualized the examples to see the tendency of the system clearly. For instance, it should be noted that the fractional derivative helped the curve represented as circular in the first derivative case, changing it from a spiral to a circular shape. On the other hand, in another case, the orbit, which initially is helical in the first derivative, becomes helical-spiral until it reaches the first derivative. Given this paper, we believe that surfaces surrounding these null points can be studied in the future, or that quaternion algebra can be used to investigate motions.

References

[1] Parker E. Acceleration of cosmic rays in solar flares, Physical Review 1957; 107(3): 830.

[2] Petschek HE. Magnetic field annihilation, in Physics of Solar Flares, edited by W. N. Ness, NASA SP-50, 1964; 425-439.

[3] Sweet PA. The Neutral Point Theory of Solar Flares, Electromagnetic Phenomena in Cosmical Physics, Proceedings from IAU Symposium no. 6. Edited by Bo Lehnert. International Astronomical Union. Symposium no. 6, Cambridge University Press, 1958; 123-134.

[4] Kostomarov DP, Echkina EY, Inovenkov IN. Bulanov SV. Simulation of magnetic reconnection in 3D geometry. Math Models Comput Simul 2, 2010; 293–303 https://doi.org/10.1134/S2070048210030038.

[5] Bolton L, Cloot AH, Schoombie SW, Slabbert JP. A proposed fractional-order Gompertz model and its application to tumour growth data. Mathematical medicine and biology: a journal of the IMA 2014; 32(2): 187-209.

[6] Dokoumetzidis A, Macheras P. Fractional kinetics in drug absorption and disposition processes. Journal of Pharmacokinetics and Pharmacodynamics, 2009; 36(2): 165-178.

[7] Popović JK, Atanacković MT, Pilipović AS, Rapaić MR, Pilipović S, & Atanacković TM. A new approach to the compartmental analysis in pharmacokinetics: fractional time evolution of diclofenac. Journal of Pharmacokinetics and Pharmacodynamics 2010; 37(2): 119-134.

[8] Baleanu D, Defterli O, Agrawal OP. A central difference numerical scheme for fractional optimal control problems. Journal of Vibration and Control 2009; 15(4): 583-597.

[9] Atangana A and Baleanu D. New fractional derivatives with nonlocal and non-singular kernel: theory and application to heat transfer model. Thermal Science 2016; 20(2): 757 763.

[10] Ozarslan R, Ercan A, Bas E. Novel Fractional Models Compatible with Real World Problems. Fractal and Fractional 2019; 3(2): 15.

[11] Bas E, Acay B, Ozarslan R. Fractional models with singular and non-singular kernels for energy efficient buildings. Chaos: An Interdisciplinary Journal of Nonlinear Science 2019; 29(2): 023110.

[12] Bas E, Ozarslan R. Real world applications of fractional models by Atangana–Baleanu fractional derivative. Chaos, Solitons & Fractals 2018; 116: 121-125.

[13] Petrás I, Magin RL. Simulation of drug uptake in a two compartmental fractional model for a biological system. Communications in Nonlinear Science and Numerical Simulation 2011; 16(12): 4588-4595.

[14] Ionescu C, Lopes A, Copot D, Machado JT, & Bates JHT. The role of fractional calculus in modeling biological phenomena: A review. Communications in Nonlinear Science and Numerical Simulation 2017; 51: 141-159.

[15] Qureshi S, Yusuf A. Fractional derivatives applied to MSEIR problems: Comparative study with real world data. The European Physical Journal Plus 2019; 134(4): 171.

[16] Qureshi S, Atangana A. Mathematical analysis of dengue fever outbreak by novel fractional operators with field data. Physica A: Statistical Mechanics and its Applications 2019; 526: 121-127.

[17] Almeida R, Qureshi S. A Fractional Measles Model Having Monotonic Real Statistical Data for Constant Transmission Rate of the Disease. Fractal and Fractional 2019; 3(4): 53.

[18] Baleanu D, Magin RL, Bhalekar S, Daftardar-Gejji V. Chaos in the fractional order nonlinear Bloch equation with delay. Communications in Nonlinear Science and Numerical Simulation 2015; 25(1-3): 41-49.

[19] Jarad F, Abdeljawad T, Baleanu D. Fractional variational optimal control problems with delayed arguments. Nonlinear Dynamics 2010; 62(3): 609-614.

[20] Jarad, F, Abdeljawad, T, Baleanu, D . Caputo-type modification of the Hadamard fractional derivatives. Advances in Difference Equations,(2012);2012(1):142.

[21] Ameen, R, Jarad, F, Abdeljawad, T . Ulam stability for delay fractional differential equations with a generalized Caputo derivative. Filomat,(2018);32(15):5265-5274.

[22] Adjabi, Y, Jarad, F, Abdeljawad, T . On generalized fractional operators and a Gronwall type inequality with applications. Filomat, (2017);31(17):5457-5473.

[23] Abdeljawad T. Fractional operators with boundary points dependent kernels and integration by parts. Discrete and Continuous Dynamical Systems - Series S, 2019; 13(3): 351-375.

[24] Has A, Yılmaz B. Effect of Fractional Analysis on Magnetic Curves, Revista Mexicana de F´ısica. 2022; 68: 1–15.

[25] Has A, Yılmaz B. Effect of fr ect of fractional analysis on some special cur actional analysis on some special curves, Turkish Journal of Mathematics 2023; 47: 1423 – 1436.

[26] Yılmaz B, A new type electromagnetic curves in optical fiber and rotation of the polarization plane using fractional calculus, Optik. 2021; 247: 168026.

[27] Yılmaz B, Has A, Obtaining fractional electromagnetic curves in optical fiber using fractional alternative moving frame, Optik. 2021; 260, 169067.

[28] Diethelm K. The analysis of fractional differential equations: An application-oriented exposition using differential operators of Caputo type. Springer Science & Business Media, 2010.

[29] Machado JT, Kiryakova V, & Mainardi F. Recent history of fractional calculus. Communications in nonlinear science and numerical simulation 2011; 16(3): 1140-1153.

[30] Loverro A. Fractional Calculus, History, Definition and Applications for the Engineer, USA, 2004.

[31] Kilbas A, Srivastava H, Trujillo J. Theory and Applications of Fractional Differential Equations, in:Math. Studies. North-Holland, New York, 2006.

[32] Garrappa R. Trapezoidal methods for fractional differential equations: Theoretical and computational aspects. Mathematics and Computers in Simulation 2015; 110: 96-112.

[33] Dumitru B, Kai D, & Enrico S. Fractional calculus: models and numerical methods, (Vol. 3). World Scientific, 2012.

[34] Struik DJ. Lectures on Classical Differential Geometry, Dover, New-York, 1988.

[35] Zhang Y. A finite difference method for fractional partial differential equation. Applied Mathematics and Computation 2009: 215(2); 524-529.

[36] Asl MS, Javidi M, Yan Y. A novel high-order algorithm for the numerical estimation of fractional differential equations. Journal of Computational and Applied Mathematics 2018; 342: 180-201.

[37] Milici C, Machado JT, Drăgănescu G. On the fractional Cornu spirals. Communications in Nonlinear Science and Numerical Simulation 2019; 67: 100-107.

[38] Has A, Yılmaz B, Akkurt A, Yıldırım H. Conformable Special Curves in Euclidean 3-Space, Filomat 36:14 (2022), 4687–4698.

[39] Has A, Yılmaz B. Special Fractional Curve Pairs with Fractional Calculus, International Electronic Journal of Geometry 2022: 15(1): 132–144.

[40] Lau TY, Finn JM, Three-dimensional Kinematic Reconnection in the Presence of Field Nulls and Closed Field Lines, The Astrophysical Journal 1990; 350: 672-691.

[41] Barros M. General Helices and a theorem of Lancert, Proceedings of the American Mathematical Society 1997; 125(5): 1503–1509.

[42] Podlubny I. Fractional differential equations: an introduction to fractional derivatives, fractional differential equations, to methods of their solution and some of their applications (Vol. 198). Elsevier, 1998.

[43] Priest ER, Forbes TG. Magnetic Reconnection, Cambridge University Press, 2000.

[44] Druţă-Romaniuc SL, Munteanu MI, Magnetic curves corresponding to Killing magnetic fields in E^3, Journal of Mathematical physics 2011; 52: 113506.

[45] Özdemir Z, Gök İ, Yaylı Y, Ekmekci FN. Notes on magnetic curves in 3D semi-Riemannian manifolds, Turkish Journal of Mathematics 2015; 39(3): 412 - 426.

[46] Bozkurt Z, Gök İ, Yaylı Y, Ekmekci FN. A new approach for magnetic curves in 3D Riemannian manifolds. Journal of Mathematical physics 2014; 55: 053501.

[47] Ceyhan H, Özdemir Z, Gök İ, Ekmekci FN. Electromagnetic Curves and Rotation of the Polarization Plane through Alternative Moving Frame. European Physical Journal Plus 2020; 135, 1.

[48] Ceyhan H, Özdemir Z, Gök İ, Ekmekci FN. A Geometric Interpretation of Polarized Light and Electromagnetic Curves Along an Optical Fiber with Surface Kinematics. Mediterr. J. Math. 2022; 19, 265.

[49] Druţă-Romaniuc SL, Munteanu MI, Killing magnetic curves in a Minkowski 3-space. Nonlinear Anal. Real World Applications. 2013; 14: 383-396.

[50] Cabrerizo JL, Magnetic fields in 2D and 3D sphere. Journal of Nonlinear Mathematical Physics 2013; 20: 440-450.